Scanning Electrochemical Microscopy: Investigation of Hydrogen Oxidation at Polycrystalline Noble Metal Electrodes

Cynthia G. Zoski*

Department of Chemistry, Georgia State University, Atlanta, Georgia 30303

Received: November 11, 2002; In Final Form: April 24, 2003

Scanning electrochemical microscopy (SECM) was used to study the kinetics of hydrogen oxidation on platinum, iridium, and rhodium substrates in acidic media. Hydrogen was generated at a platinum tip by reduction of H^+ and oxidized at a Pt, Ir, or Rh substrate. The Tafel slope (117 mV, corresponding to a transfer coefficient, α, of 0.50) and the rate constant for hydrogen oxidation on Pt obtained by fitting approach curves (0.22 cm/s at the halfwave potential) agree with a previous SECM result. Kinetic data were also obtained on Ir (Tafel slope = 113 mV, k° = 0.25 cm/s, α = 0.48), and Rh (Tafel slope = 138 mV, k° = 0.010 cm/s, α = 0.58) substrates. These results demonstrate that hydrogen oxidation on Pt and Ir occurs at a similar rate, but is much slower on Rh.

1. Introduction

The electrochemical oxidation of molecular hydrogen has been the subject of extensive investigations over the last century. This is largely because the H_2 oxidation reaction is important to energy conversion, specifically in the area of fuel cells where it has practical utility as an anode reaction.[1−3] Much effort has been devoted to understanding the kinetics and mechanism of this reaction in an attempt to search for low-cost and more efficient electrocatalysts for H_2 oxidation which would have widespread application in fuel cells and many other electrochemical applications. For example, platinum has received the greatest attention as a result of the high catalytic hydrogen oxidation rate that can be obtained at an unoxidized Pt surface. The other noble metals of the Pt family, which include Ir, Pd, Rh, and Ru, have been studied to a lesser degree but are frequently used as catalyst components.[4−6]

Hydrogen oxidation at electrodes requires a catalytic surface on which H atoms are adsorbed and is observed only with metals such as Pt, Pd, Rh, Ru, and Ir. On polycrystalline metal surfaces, it is now generally accepted that H_2 oxidation at room temperature is a fast process that proceeds by initial adsorption of molecular hydrogen, which involves either slow dissociation of H_2 molecules into atoms (reaction 1) or dissociation into the ion and atom (reaction 2) followed by a charge-transfer step (reaction 3):[6]

***Tafel*:** $H_2 \xrightarrow{\text{RDS}} 2H(a)$ Tafel slope = 30 mV (1)

***Heyrovsky*:** $H_2 \xrightarrow{\text{RDS}} H(a) + H^+ + e$ Tafel slope = 120 mV (2)

***Volmer*:** $H(a) \xrightarrow{\text{RDS}} H^+ + e$ Tafel slope = 120 mV (3)

where H(a) represents atomic hydrogen that is chemisorbed to a metal surface. Reactions 1−3 are historically referred to as the Tafel−Volmer (steps 1 and 3) and Heyrovsky−Volmer (steps 2 and 3) sequences, respectively, where the Tafel and Heyrovsky steps are generally believed to be the rate-determining steps (RDS). From a steady-state current−potential curve, a plot of log i versus overpotential leads to a Tafel plot from which a slope of $(1 - \alpha)nF/RT$ and a value of the transfer coefficient α are generally calculated. The exchange current is obtained from an extrapolation to an intercept of log i_o.[7] In a number of past studies of platinum concerning the hydrogen oxidation reaction, a Tafel slope of 30 mV was found, lending support to a Tafel−Volmer mechanism, although this generated a great deal of controversy that still continues.[3,6]

Methods of investigating the hydrogen oxidation reaction have included cyclic voltammetry,[8−11] rotating disk voltammetry,[6,12−17] steady-state experiments with intensive bubbling of hydrogen,[18,19] and more recently, scanning electrochemical microscopy (SECM).[20−23] Cyclic voltammetric experiments are plagued by ohmic drop in solution and by high charging currents at the sweep rates necessary to probe the kinetics of very fast reactions.[24] Rotating disk methods are limited in ability to access high rate constants by the onset of turbulent flow and vortex formation at rotation rates in excess of 10 000 rpm.[25] In SECM,[26,27] an ultramicroelectrode (UME), called the tip, is scanned toward the surface of a biased substrate. A plot of the tip current, i_T, as a function of distance, d, between the tip and the substrate, is called an approach curve. The effect of substrate potential on i_T can be used to obtain information about the heterogeneous kinetics on the substrate. The steady-state kinetic measurements possible with SECM have been demonstrated to be comparatively free from complications caused by ohmic drop, double-layer charging, and mechanical difficulties that are associated with the other electrochemical techniques traditionally used to study hydrogen oxidation.[28,29] Moreover, rotation rates in excess of 10^6 rotations per minute would be required to attain the large effective mass-transfer rate constants obtainable with SECM. Additionally, the UMEs used in this study and other similar studies are of dimensions that are now considered routine in terms of fabrication or, alternatively, they are commercially available. Thus, SECM has been shown to be a practical and alternative method in probing reactions with fast heterogeneous reaction rates.[26−29]

In this paper, SECM was used to study hydrogen oxidation on platinum, iridium, and rhodium in acid media. Figure 1 illustrates the basic principle of the feedback mode of SECM

* E-mail: checgz@panther.gsu.edu.

10.1021/jp027436g CCC: $25.00
Published on Web 06/05/2003

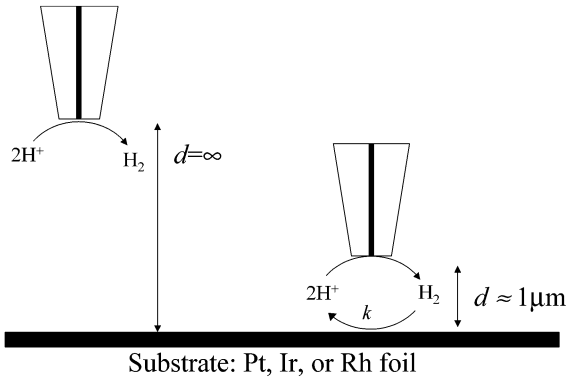

Figure 1. Feedback mode of SECM used in the study of H^+ oxidation in acid solution.

used in the present work. Protons are reduced at the tip, and the tip potential is adjusted to reduce H^+ at a diffusion-controlled rate. When the tip is far away from the substrate (Pt, Ir, or Rh), a steady-state current, $i_{T,\infty}$ flows. This current results from the hemispherical diffusion of H^+ to the tip. As the tip is brought within a few tip radii of the substrate, the H_2 generated at the tip diffuses to the substrate where it can be oxidized. This process generates H^+ at the substrate and produces an enhancement in the faradic current at the tip electrode, depending on the tip/substrate separation and the rate of reaction at the substrate. Quantitative theory has been developed for different modes of the SECM operation and kinetic parameters of H_2 oxidation can be extracted by fitting experimental tip current versus distance (approach curves) to theory.[26,27]

2. Experimental Section

2.1. Chemicals. Perchloric acid (Aldrich, 70%, redistilled 99.999%. DANGER: corrosive; causes digestive and respiratory tract burns; causes eye and skin burns; strong oxidizer; contact with other material may cause a fire.) and sodium perchlorate (Aldrich, ACS reagent, 99%) were used as received. Solutions were prepared with deionized water (Milli-Q, Millipore Corp.) and deaerated with argon (Specialty Gases Southeast) prior to and between measurements.

2.2. Electrodes. Pt foil (0.25 mm thick, 99.9% purity), Ir foil (0.127 mm thick, 99.8% purity), and Rh foil (0.1 mm thick, 99.8% purity) were used as the substrate. To achieve a mirror finish, each foil was initially polished with emory paper (Buehler: 400, 600, 800, and 1200 grit) followed by alumina (Buehler: 1, 0.3, 0.05 μm) on polishing cloth (Buehler, microcloth). Before each experiment, each foil was polished with 800 and 1200 grit emory paper and 1, 0.3, 0.05 μm alumina, followed by rinsing in deionized water, and sonicating in a methanol/water solution and last in deionized water. The foils were dried with a stream of argon. Each foil contacted the solution through a 6 mm inner diameter Teflon O-ring (McMaster-Carr, size 010). Foil pretreatment was achieved by electrochemical potential cycling in 1 M $HClO_4$/0.1 M $NaClO_4$ from -0.27 to 1.3 V vs SCE for Pt, -0.29 to 0.8 V vs SCE for Rh, and -0.26 to 0.7 V vs SCE for Ir until reproducible cyclic voltammograms were obtained. The oxide region was avoided for Ir and Rh foils because of the thick and irreversible nature of the oxide films which can develop at these metal surfaces during cycling.[4,5,30−32]

Pt SECM tips (25 μm diameter) were purchased from CH Instruments. For the tips used in this work, RG was maintained at $\cong 5$. The tip was initially polished with 1 and 0.05 μm alumina, followed by rinsing in deionized water, and sonicating in methanol/water and in deionized water. Before each experiment, the tip was polished with 0.05 μm alumina and sonicated in methanol/water and last in deionized water. All potentials are referenced against the SCE reference electrode (CH Instruments, saturated KCl, double fritted). A platinum wire (Alfa Aesar, 0.5 mm diameter) was used as the auxiliary electrode.

2.3. Electrochemical Measurements. A CHI 900 SECM (CH Instruments, Austin, TX) was used for SECM experiments, and a CHI 660a Electrochemical Workstation (CH Instruments, Austin, TX) was used for proton reduction cyclic voltammetric scans where IR compensation was needed. All experiments were performed in a Teflon cell ($\approx$ 3 mL). The solution was deaerated with argon. Before each approach curve in 0.01 M $HClO_4$/0.10 M $NaClO_4$ was recorded, the potential of the Pt tip was cycled between -0.36 and 1.3 V vs SCE and the potential of the substrate electrode was cycled between -0.36 and 1.3 V vs SCE for Pt, -0.37 and 0.8 V vs SCE for Ir, and -0.35 and 0.7 V vs SCE for Rh until reproducible cyclic voltammograms characteristic of polycrystalline Pt, Ir, and Rh were obtained. The approach curves were obtained by setting the tip potential at -0.8 V vs SCE (i.e., at the diffusion limiting current of H^+ reduction). The tip−substrate distance was found by calibration with approach curves in the region where the positive feedback was the greatest for each substrate surface. All experiments were carried out at room temperature.

3. Results and Discussion

3.1. Voltammetry of Hydrogen Ion on Electrode Surfaces. Reproducible surface behavior at a 25 μm diameter Pt tip electrode in a deaerated solution of 10 mM $HClO_4$ was obtained by cycling the potential between values corresponding to hydrogen adsorption and water oxidation until reproducible behavior was obtained, as shown in Figure 2a. A typical cyclic voltammogram (CV) as shown in Figure 2b resulted at the platinum tip microelectrode, consistent with previous studies of the voltammetry of hydrogen ion in aqueous solutions on platinum microelectrodes.[20,21,33] A steady-state current was obtained at potentials more negative than -0.6 V, indicating a diffusion-controlled current produced by proton reduction

$$2H^+ + 2e \rightarrow H_2 \tag{4}$$

This limiting current is given by

$$i_{T,\infty} = 4nFDca \tag{5}$$

where n is the electron-transfer number (=1 for proton reduction), F is the Faraday constant, D is the diffusion coefficient, c is the concentration of the reactant, and a is the radius of the microdisk. The measured current, i_T, is often normalized by $i_{T,\infty}$ and this is expressed as $I = i_T/i_{T,\infty}$. An acid concentration of 10 mM has been shown to be well below the concentration limit for the onset of hydrogen bubble formation.[20]

Figure 3 shows CVs which resulted from cycling the potential at Pt, Ir, and Rh foils until reproducible waves were obtained. These CVs are consistent with previous studies which show a similar hydrogen adsorption range (0 to -0.35 V vs SCE) and multiple hydrogen adsorption peaks in the cathodic and anodic hydrogen region for Pt and Ir.[4] In contrast, hydrogen adsorption commences at significantly more negative potentials (-0.1 to -0.35 V vs SCE) on Rh, and a single hydrogen adsorption/desorption peak is observed in the cathodic and anodic hydrogen region so that the hydrogen is said to be more weakly bonded.[4] Oxide formation on Pt begins at approximately 0.4 V vs SCE, while for Ir and Rh it begins at approximately 0.2 V vs SCE.[4]

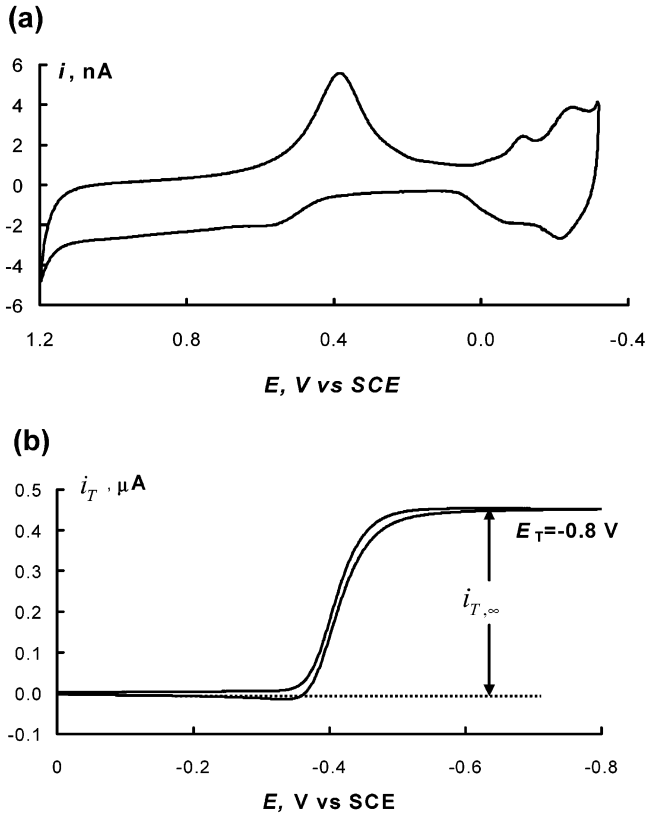

Figure 2. Voltammograms for a 10 mM deaerated solution of perchloric acid, recorded with a freshly polished platinum disk electrode of 25 μm diameter. (a) Cyclic voltammogram recorded after activating the Pt surface. (b) Steady-state voltammogram. The solution also contained 0.1 M $NaClO_4$. The scan rate was 100 mV/s.

Figure 4 shows the CV for proton reduction at each of the foils after potential cycling. The cathodic peak corresponds to proton reduction and the anodic wave corresponds to the oxidation of hydrogen.

3.2. Hydrogen Oxidation on Pt, Ir, and Rh. In SECM, the rate constants for heterogeneous electron transfer on substrates can be measured by fitting approach curves with SECM theory for a process governed by finite substrate heterogeneous kinetics.[34,35] The following equations were used to extract the first-order effective heterogeneous electron-transfer rate constant:

$$I_T^k = I_S^k(1 - I_T^{ins}/I_T^c) + I_T^{ins} \quad (6)$$

$$I_S^k = 0.78377/L(1 + 1/\Lambda) + [0.68 + 0.3315\exp(-1.0672/L)]/[1 + F(L,\Lambda)] \quad (7)$$

Here, I_T^k, I_T^{ins}, and I_T^c represent the normalized tip currents for finite substrate kinetics, insulating substrate (i.e., no H^+ regeneration), and diffusion-controlled regeneration of H^+, respectively, at a normalized tip−substrate separation, $L = d/a$. I_S^k is the kinetically controlled substrate current where $\Lambda = kd/D$ and $F(L,\Lambda) = (11 + 7.3\Lambda)/[\Lambda(110 - 40L)]$ with k as the apparent heterogeneous rate constant (cm/s), and the diffusion coefficient $D = 7.1 \times 10^{-5}$ cm^2 s^{-1}.[20] The analytical approximations for I_T^c and I_T^{ins} are

$$I_T^c = 0.78377/L + 0.3315\exp(-1.0672/L) + 0.68 \quad (8)$$

$$I_T^{ins} = 1/(0.15 + 1.5358/L + 0.58\exp(-1.14/L) + 0.0908\exp[(L - 6.3)/(1.017L)]) \quad (9)$$

These equations are valid over the range $-2 \le \log \Lambda \le 3$.

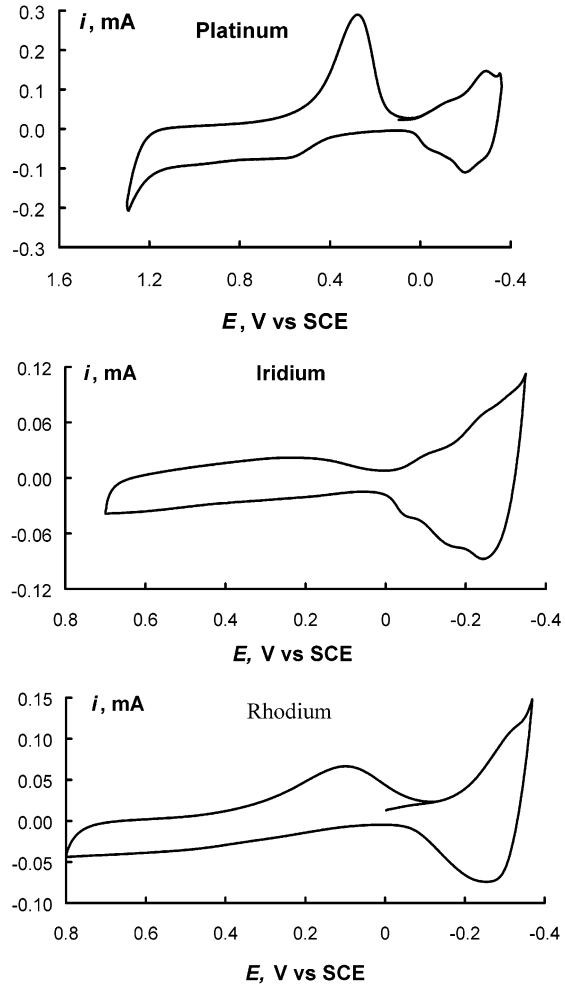

Figure 3. Cyclic voltammograms recorded with platinum, iridium, and rhodium foils of 6 mm exposed diameter in a solution of 10 mM perchloric acid and 0.1 M $NaClO_4$ at 100 mV/s after potential cycling.

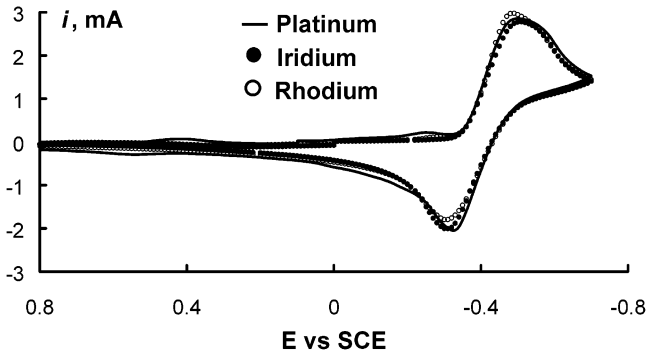

Figure 4. Proton reduction at platinum, iridium, and rhodium foils of 6 mm exposed diameter in a solution of 10 mM perchloric acid and 0.1 M $NaClO_4$ at 100 mV/s.

To measure the H_2 oxidation rate on platinum, iridium, and rhodium substrates, approach curves were obtained by setting the potential of the Pt tip to −0.8 V where diffusion-controlled H_2 evolution occurs at the tip, and then moving the tip toward the substrate, held at different potentials. At each substrate, a family of approach curves was recorded, starting at the most negative potential and moving incrementally toward positive potentials. In this way, hydrogen oxidation rates could be measured in the absence of oxide layers. Figure 5 shows approach curves at different substrate potentials as well as theoretical curves for a diffusion-controlled reaction (conductor behavior) and no reaction (insulator behavior) at the substrate.

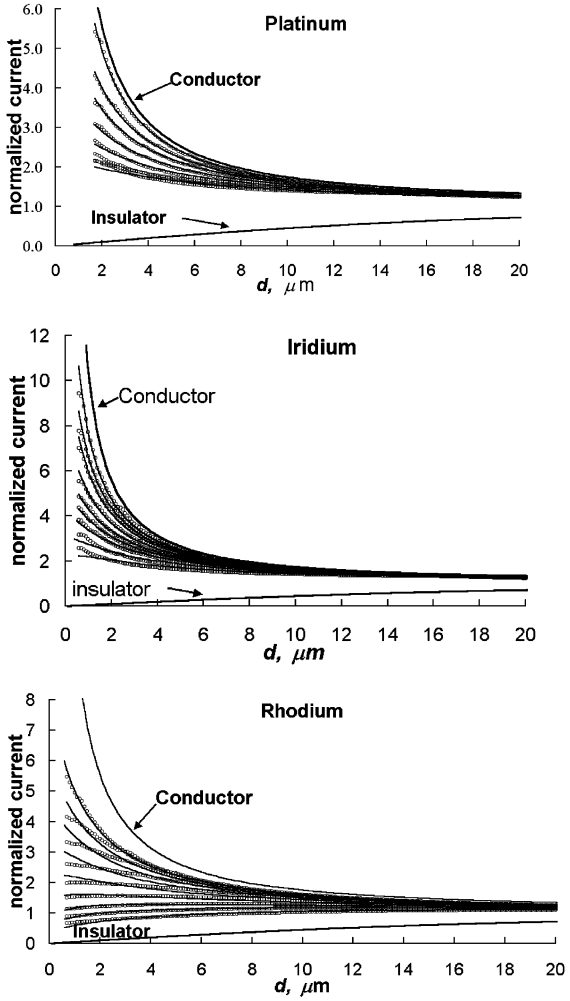

Figure 5. SECM approach curves obtained on platinum, iridium, and rhodium substrates with the platinum tip potential held at −0.8 V. The tip was a 12.5 μm radius Pt microdisk. The aqueous solution was 10 mM in perchloric acid and 0.1 M $NaClO_4$. Approach speed was 3 μm/s. The solid lines are theoretical approach curves, and the open circle symbols are experimental approach curves at substrates with potential held at (from top to bottom) (a) platinum: −300, −350, −375, −390, −410, −430, −440 mV vs SCE; (b) iridium: −300, −340, −350, −370, −380, −390, −400, −420, −440 mV vs SCE; (c) rhodium: −75, −175, −200, −225, −250, −275, −300, −325, −350 mV vs SCE.

Before the tip approached the substrate, both the tip and substrate potentials were cycled until reproducible CV waves were observed (Figures 2a and 3). The rate constant for the heterogeneous oxidation of hydrogen on Pt, Ir, or Rh was then obtained by fitting the approach curves to the theoretical ones and plotted versus substrate potential as shown in Figure 6.

Platinum and iridium are similar in behavior to hydrogen oxidation as shown in Figure 6a. Between −0.43 and −0.35 V, the H_2 oxidation rate increased with an increase in substrate potential. Figure 7, equivalent to a Tafel plot, is a plot of the H_2 oxidation rate from the approach curves versus overpotential. The halfwave potential (−0.41 V) from the steady-state voltammogram at the tip was taken as the equilibrium potential, E_{eq}, to calculate the overpotential. Over this potential range, the Tafel plot was a straight line, with a slope of 117 mV (log $k = 0.0086\ mV^{-1}\eta - 0.6502$) for platinum and a slope of 113 mV (log $k = 0.0089 mV^{-1}\eta - 0.6068$) for iridium, close to a typical Tafel slope of 118 mV. The slope corresponds to a transfer coefficient, α, of 0.50 for platinum and 0.48 for iridium. In contrast, the hydrogen oxidation rate on rhodium (Figure 6b) increases from −0.35 to −0.225 V, with the heterogeneous rate of hydrogen

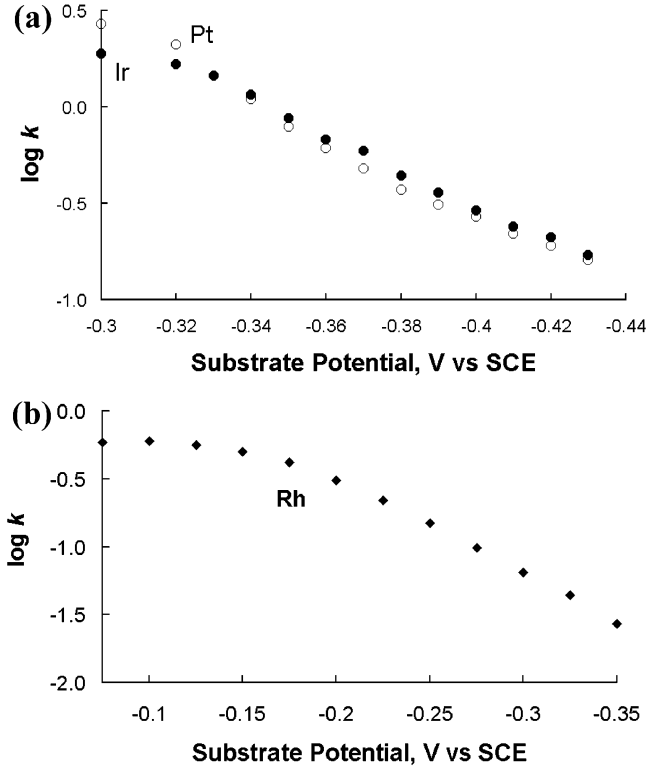

Figure 6. Heterogeneous reaction rate constant k of H_2 oxidation at (a) platinum (○) and iridium (●) and (b) rhodium (◆) substrates with different potentials. k was obtained by fitting the experimental approach curves with the theoretical ones as shown in Figure 5.

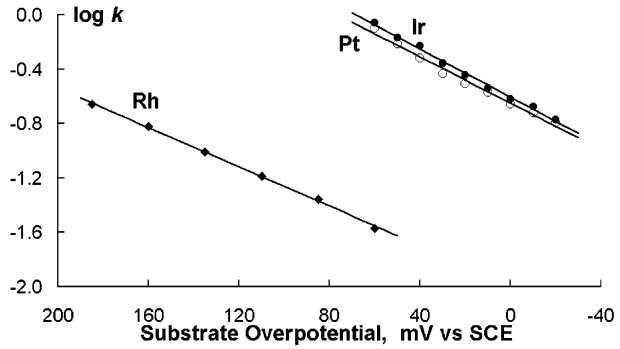

Figure 7. Tafel plot of H_2 oxidation on platinum (○), iridium (●), and rhodium (◆) substrates. The solid lines represent a linear least-squares fit through the experimental points.

oxidation being approximately one log unit below that found for platinum and iridium. Over this potential range, the Tafel plot (Figure 7) was a straight line, with a slope of 138 mV (log $k = 0.0072 mV^{-1}\eta - 1.9868$) which corresponds to an α of 0.58. By extrapolating the lines in the Tafel plot to $E = E_{eq}$, standard heterogeneous rate constants of 0.22 cm/s (platinum), 0.25 cm/s (iridium), and 0.010 cm/s (rhodium) were found.

When the substrate potential was more positive than −0.35 V for platinum and iridium, the rate constant approached a limiting value (Figure 6a) greater than 2 cm/s which has been shown to be indicative of mass transfer control.[20] This is not the case for rhodium, however. At potentials more positive than −0.2 V, the rate constant reached a constant value of 0.6 cm/s, indicating that in this potential range the rate-determining step is likely to be a chemical process, such as the dissociative adsorption of H_2, prior to the slower electron-transfer step.

Because the focus of this work concerned solely the kinetics of the hydrogen oxidation reaction, SECM measurements were

not attempted beyond potentials where limiting behavior was found for rate constants determined from approach curves (Figure 6). These potentials corresponded to −0.3 V for platinum and iridium, and −0.075 V for rhodium. Potentials more positive than any one of these, lead to regions involving oxide coverage (Figure 3) where oxidation of H_2 has been shown to decrease.[20,22]

3.3. Comparison with Literature. The Tafel slopes of 117 mV (Pt), 113 mV (Ir), and 138 mV (Rh) obtained in this work imply that the rate-determining step in hydrogen oxidation is either the Herovsky (reaction 2) or the Volmer (reaction 3) reaction. The Tafel slope on platinum, in addition to a standard rate constant of 0.22 cm/s and a transfer coefficient of 0.50 also found in this work, are in good agreement with a similar study on polycrystalline platinum where a Tafel slope of 117 mV, $k^\circ = 0.42$ cm/s, and $\alpha = 0.50$ were also found.[20] In another SECM study on polycrystalline platinum, a Tafel slope of 30 mV was reported.[22] The majority of investigations involving hydrogen oxidation at polycrystalline surfaces have employed some sort of convection either by bubbling of hydrogen and/or by rotating disk methods.[6] In such studies, Tafel slopes of 30 mV (platinum), 50 mV (iridium), and 38 mV (rhodium) have been determined, and it has been suggested that hydrogen oxidation proceeds through a Tafel−Volmer sequence with the Tafel reaction as the rate-determining step.[6]

Standard rate constants of 0.22 cm/s (Pt), 0.25 cm/s (Ir), and 0.010 cm/s (Rh) determined in this work indicate similar catalytic activity of Pt and Ir in response to H_2 oxidation, and much slower catalytic activity from Rh. In searching the literature, it is more usual to find values of exchange current density than values of standard rate constants in electrocatalytic investigations. Because exchange current densities depend on concentrations of reactants, a direct comparison cannot be made unless the concentrations are the same. Moreover, very few studies have been reported on either iridium or rhodium which lead to reported values of exchange current densities. However, one study reports exchange current densities of 1.9 A/cm^2 (Pt), 0.40 A/cm^2 (Ir), and 0.30 A/cm^2 (Rh),[6] suggesting that hydrogen oxidation on Ir and Rh is similarly slow compared to that on Pt. These results do not agree with the comparative standard rate constants of this work nor with previous studies demonstrating similar catalytic behavior of Pt and Ir.[36]

4. Conclusions

The feedback mode of SECM was used to study the kinetics of hydrogen oxidation on Pt, Ir, and Rh substrates in acid media. A Pt ultramicroelectrode, on which a well-defined reduction wave of H^+ was obtained, was used as the SECM tip. SECM approach curves were then used to study hydrogen oxidation on Pt, Ir, and Rh substrates.

The Tafel slope and rate constant for H_2 oxidation on Pt are in agreement with an earlier study using SECM. Results from this work also indicate similar hydrogen oxidation kinetics on Pt and Ir, and much slower kinetics on Rh. This comparative reactivity to hydrogen oxidation is in general agreement with that obtained by other researchers. The Tafel slopes for H_2 oxidation on Pt, Ir, and Rh obtained in this work suggest that the rate-determining step could be either the Heyrovsky or the Volmer reactions.

Acknowledgment. Funding from the National Science Foundation (CHE-0210315) and Georgia State University Research Initiation Grant are greatly appreciated.

References and Notes

(1) Markovic, N. M.; Ross, P. N. In *Interfacial Electrochemistry: Theory, Experiment, and Applications*; Wieckowski, A., Ed.; Marcel Dekker: New York, 1999; pp 821−841.
(2) Ohms, D.; Plzak, V.; Trasatti, S.; Wiesener, K.; Wendt, H. In *Electrochemical Hydrogen Technologies*; Wendt, H., Ed.; Elsevier: Amsterdam, 1990; pp 1−4.
(3) Lipkowski, J.; Ross, P. N. *Electrocatalysis: Frontiers of Electrochemistry*; Wiley-VCH Publishers: New York, 1998.
(4) Woods, R. In *Electroanalytical Chemistry*; Bard, A. J., Ed.; Marcel Dekker: New York, 1976; Vol. 9, pp 1−162.
(5) Conway, B. E. In *Electrodes of Conductive Metallic Oxides, Part B*; Trasatti, S., Ed.; Elsevier: Amsterdam, 1981; pp 433−519.
(6) Conway, B. E.; Tilak, B. V. *Electrochim. Acta* **2002**, *47*, 3571.
(7) Bard, A. J.; Faulkner, L. R. *Electrochemical Methods: Fundamentals and Applications*; Wiley: New York, 2001; Chapter 3.
(8) Angerstein-Kozlowska, H.; Conway, B. E. *J. Electroanal. Chem.* **1979**, *95*, 1.
(9) Breiter, M. W. *Ann. N.Y. Acad. Sci.* **1963**, *101*, 709.
(10) Breiter, M. W. *Electrochim. Acta* **1963**, *8*, 973.
(11) Capon, A.; Parsons, R. *J. Electroanal. Chem.* **1972**, *39*, 275.
(12) Bagotzky, V. S.; Osetrova, N. V. *J. Electroanal. Chem.* **1973**, *43*, 233.
(13) Makowski, M.; Heitz, E.; Yeager, E. *J. Electrochem. Soc.* **1966**, *113*, 204.
(14) Harrison, J. A.; Khan, Z. A. *J. Electroanal. Chem.* **1971**, *30*, 327.
(15) Gasteiger, H. A.; Markovic, N. M.; Ross, P. N. *J. Phys. Chem.* **1995**, *99*, 8945.
(16) Grgur, B. N.; Markovic, N. M.; Ross, P. N. *J. Phys. Chem. B* **1998**, *102*, 2494.
(17) Markovic, N. M.; Grgur, B. N.; Ross, P. N. *J. Phys. Chem. B* **1997**, *101*, 5405.
(18) Schuldiner, S. *J. Electrochem. Soc.* **1968**, *115*, 362.
(19) Schuldiner, S. *J. Electrochem. Soc.* **1969**, *116*, 767.
(20) Zhou, J.; Zu, Y.; Bard, A. J. *J. Electroanal. Chem.* **2000**, *491*, 22.
(21) Shah, B. C.; Hillier, A. C. *J. Electrochem. Soc.* **2000**, *147*, 3043.
(22) Jambunathan, K.; Shah, B. C.; Hudson, J. L.; Hillier, A. C. *J. Electroanal. Chem.* **2001**, *500*, 279.
(23) Jayaraman, S.; Hillier, A. C. *Langmuir* **2001**, *17*, 7857.
(24) Bard, A. J.; Faulkner, L. R. *Electrochemical Methods: Fundamentals and Applications*; Wiley: New York, 2001; Chapters 6, 12.
(25) Bard, A. J.; Faulkner, L. R. *Electrochemical Methods: Fundamentals and Applications*; Wiley: New York, 2001; Chapters 8, 12.
(26) Bard, A. J.; Fan, F.-R. F.; Mirkin, M. V. In *Electroanalytical Chemistry*; Bard, A. J., Ed.; Marcel Dekker: New York, 1994; Vol. 18, pp 243−373.
(27) *Scanning Electrochemical Microscopy*; Bard, A. J., Mirkin, M. V., Eds.; Marcel Dekker: New York, 2001.
(28) Mirkin, M. V.; Richards, T. C.; Bard, A. J. *J. Phys. Chem.* **1993**, *97*, 7672.
(29) Mirkin, M. V.; Bulhoes, L. O. S.; Bard, A. J. *J. Am. Chem. Soc.* **1993**, *115*, 201.
(30) Llopis, J. F.; Colom, F. In *Encyclopedia of Electrochemistry of the Elements*; Bard, A. J., Ed.; Marcel Dekker: New York, 1976; Vol. 6, pp 221−234.
(31) Llopis, J. F.; Tordesillas, I. M. In *Encyclopedia of Electrochemistry of the Elements*; Bard, A. J., Ed.; Marcel Dekker: New York, 1976; Vol. 6, pp 299−329.
(32) Hoare, J. P. *The Electrochemistry of Oxygen*; Interscience Publishers: Wiley: New York, 1968.
(33) Daniele, S.; Lavagnini, I.; Baldo, M. A.; Magno, F. J. *J. Electroanal. Chem.* **1996**, *404*, 105.
(34) Bard, A. J.; Mirkin, M. V.; Unwin, P. R.; Wipf, D. O. *J. Phys. Chem.* **1992**, *96*, 1861.
(35) Wei, C.; Bard, A. J.; Mirkin, M. V. *J. Phys. Chem.* **1995**, *99*, 16033.
(36) Breiter, M. W. *Electrochemical Processes in Fuel Cells*; Springer-Verlag: New York, 1969; pp 78−90.